INTERNATIONAL JOURNAL FOR NUMERICAL AND ANALYTICAL METHODS IN GEOMECHANICS, VOL. 22, 29–48 (1998)

A MODEL FOR COUPLED MECHANICAL AND HYDRAULIC BEHAVIOUR OF A ROCK JOINT

T. S. NGUYEN[1] AND A. P. S. SELVADURAI[2]*

[1] *Atomic Energy Control Board, 280 Slater, Ottawa, Canada, K1P 5S9*
[2] *McGill University, 817 Sherbrooke West, Montreal, Canada, H3A 2K6*

SUMMARY

Constitutive laws for rock joints should be able to reproduce the fundamental mechanical behaviour of real joints, such as dilation under shear and strain softening due to surface asperity degradation. In this work, we extend the model of Plesha[1] to include hydraulic behaviour. During shearing, the joint can experience dilation, leading to an initial increase in its permeability. Experiments have shown that the rate of increase of the permeability slows down as shearing proceeds, and, at later stages, the permeability could decrease again. The above behaviour is attributed to gouge production. The stress–strain relationship of the joint is formulated by appeal to classical theories of interface plasticity. It is shown that the parameters of the model can be estimated from the Barton–Bandis empirical coefficients; the Joint Roughness Coefficient (JRC) and the Joint Compresive strength (JSC). We further assume that gouge production is also related to the plastic work of the shear stresses, which enables the derivation of a relationship between the permeability of the joint and its mechanical aperture. The model is implemented in a finite element code (FRACON) developed by the authors for the simulation of the coupled thermal–hydraulic–mechanical behaviour of jointed rock masses. Typical laboratory experiments are simulated with the FRACON code in order to illustrate the trends predicted in the proposed model. © 1998 by John Wiley & Sons. Ltd.

Int. J. Numer. Anal. Meth. Geomech., Vol. 22, 29–48 (1998)
(No. of Figures: 16 No. of Tables: 0 No. of Refs: 39)

Key words: hydraulic behaviour; joint; mechanics of joint; joint degradation; joint elements; interface mechanics

INTRODUCTION

Discontinuities in rock masses, which shall be referred to as 'joints' in this paper, constitute planes of weakness in the rock mass from the point of view of its mechanical behaviour. Under external loads, sliding along the joints is likely to occur. Due to the presence of asperities at the joint surfaces, dilation usually accompanies the shearing process, leading to an increase in the joint aperture. As a consequence, the joint becomes more permeable. The asperities of the joint walls have finite strength. Mechanical degradation of these asperities occurs during shear, and the dilation of the joint will diminish at the later stages of the shearing process. During this process, gouge material is being produced by the damage of the asperities and the accumulation of the gouge material can result in the reduction of flow in the joint. The very limited number of

*Correspondence to A. P. S. Selvadurai, McGill University, 817 Sherbrooke Street West, Montreal, Canada, H3A 2K6

CCC 0363–9061/98/010029–20$17.50

Received 30 March 1995
Revised 4 April 1997

experiments[2–4] which investigate the effects of shear on joint permeability show that as shearing proceeds, the permeability decreases as a result of gouge production.

Patton[5] performed experiments on artificial joints with regular 'saw-tooth' shapes moulded out of plaster of Paris. He proceeded to propose a bilinear model of a shear strength criterion; at low normal stress, the joint shows dilation during shear due to overriding of the asperities; at high normal stress, shear through the asperities occurs and limited dilation is observed. Ladanyi and Archambault,[6] Jaeger,[7] Barton and Choubey[8] and Bandis *et al.*[9] proposed similar strength criteria, with a smooth transition between the two extreme types of response proposed by Patton.[4] Barton and Choubey,[7] and Bandis *et al.*[8] introduce the empirical coefficients JRC (Joint Roughness Coefficient) and JCS (Joint Compressive Strength) in their strength criterion. These empirical coefficients are easily determined either in the laboratory or *in situ* and they are a measure of the roughness of the joint surface (JRC) and the strength of the asperities (JCS). Empirical relations are proposed by these authors in order to include scale-dependency of JRC and JCS. The above strength criteria delineate the state of stress that separates pre-sliding and post-sliding of the joints. In order to predict the stress–strain behaviour of joints in both stages, numerous constitutive relationships have been proposed. These relationships could be categorized into two main classes. The incremental relationships[10–15] consist of piecewise linear relationships between the increment of stress and the increment of strain. These relationships are usually developed from direct shear tests under constant normal stress and their use under different load paths is not straightforward. Graphical methods to use these models to predict shear behaviour under constrained dilation (or constant normal stiffness) have been proposed with some success.[16–18] Boulon and Nova[15] and Benjelloun[4] proposed an incremental approach with directional dependency. In this approach, the stress–strain matrices are determined from elementary stress paths derived from laboratory tests (such as shear under constant normal stress conditions). A weighted interpolation procedure between the elementary stress paths is used to determine the incremental stress–strain matrix for other stress paths. The second category of constitutive relationships are the elastoplastic relationships, derived from the theory of plasticity. The models which fall into this category assume that before sliding, the deformations are elastic (recoverable). Post-sliding behaviour is characterized by plastic (irrecoverable) deformations. The state of stress that separates elastic from plastic behaviour is defined by appeal to a yield criterion. For example, Roberds and Einstein[19] used the strength criterion proposed by Patton[5] as the yield criterion to formulate their elastoplastic model. Strain-softening (decrease in shear stress in the plastic stage) often found in experimental behaviour of joints could not be predicted from the model proposed by Roberds and Einstein.[19] Numerous elastoplastic models exist in the literature (see, e.g. References 1 and 19–23, to name only some). The elastoplastic approach has a particular appeal since different load paths and directions could be accommodated. Among the above models, the one proposed by Plesha[1] is particularly attractive due to its simplicity and its ability to capture certain fundamental aspects of the mechanical behaviour of real joints, such as dilation under shear and strain softening due to surface asperity degradation.

For predicting the hydraulic behaviour of rock joints, the parallel plate model, developed from the application of the Navier–Stokes equation for laminar incompressible flow between two parallel smooth plates, is widely used to calculate the effective permeability k of a fracture (see, e.g. Reference 4). The permeability of the joint is thus expressed as a function of its effective opening to fluid flow, called the hydraulic aperture. Since natural fractures are quite dissimilar to ideal parallel plates, the hydraulic aperture of the fracture is not equal to its mechanical aperture. Empirical relationships between the mechanical and hydraulic apertures were proposed by

Barton,[24] Elliot *et al.*,[25] Witherspoon *et al.*[26] and Benjelloun.[4] The effect of gouge production on the permeability of the joint, however, is not accounted for in these relationships.

In this paper, we employ the classical plasticity theory based on the methodology proposed by Plesha[1] to formulate the stress–strain relationship for a joint. We show how the parameters of the above constitutive relationship could be estimated from two widely used and easily measurable empirical coefficients, the JRC and JCS. In order to derive a relationship between the permeability of the joint and its mechanical aperture, we further assume that gouge production is related to the plastic work. A finite element code FRACON (FRACtured medium CONsolidation) for simulating the coupled thermal–hydraulic–mechanical behaviour of jointed rock masses had been developed by the authors. The extended version of the model proposed by Plesha[1] is implemented in the code. Laboratory experiments available in the literature are simulated with the FRACON code in order to illustrate the trends predicted by the proposed model. The focus of this paper is restricted to joints without infilling material. Temperature effects on the strength of the joint are assumed to be negligible. Based on the experimental data obtained by Stesky *et al.*,[27] this seems to be a justifiable assumption, at least for temperatures below 100°C.

ELASTOPLASTIC MODELLING OF THE MECHANICAL BEHAVIOUR OF A JOINT

Patton's saw-tooth model

The surface asperities of dilatant rock joints are irregular in shape and height. Nevertheless, their basic mechanical behaviour could be explained by assuming an idealized two-dimensional saw-tooth pattern as proposed by Patton.[5] This idealization is adopted by Plesha[1] and several other researchers (e.g. References 19, 30 and 38). Thus it is useful to review the basic concept of the model attributed to Patton.[5]

Consider a joint with perfectly planar contact surfaces (Figure 1), subjected to a normal stress σ and a shear stress τ. Sliding will not occur if:

$$|\tau| < -\sigma \tan \phi \tag{1}$$

where $\tan \phi$ is the coefficient of friction between the two contact planes and tensile normal stresses are considered positive. This is the basic Coulomb model for non-dilatant behavior.

The yield criterion required for the theory of plasticity is defined as

$$F(\tau, \sigma) = |\tau| + \sigma \tan \phi \tag{2}$$

such that when $F = 0$, sliding results in irrecoverable (plastic) deformation.

We introduce the relative displacement between the two adjoining planes, respectively, $u = u_1$, in the shear direction (direction 1) and $v = u_2$, in the normal direction (direction 2). When $F = 0$, increments of stress will result in increments of plastic deformations. In order to determine the direction and magnitude of plastic deformation, we define a plastic potential function $Q = Q(\tau, \sigma)$ such that

$$\mathrm{d}u_i^{\mathrm{p}} = \mathrm{d}\lambda \frac{\partial Q}{\partial \sigma_i} \tag{3}$$

where $i = 1, 2$; $\sigma_1 = \tau$ and $\sigma_2 = \sigma$, $\mathrm{d}u_i^{\mathrm{p}}$ are the plastic components of the relative displacement at the surface of the joint and $\mathrm{d}\lambda$ is a scalar multiplier.

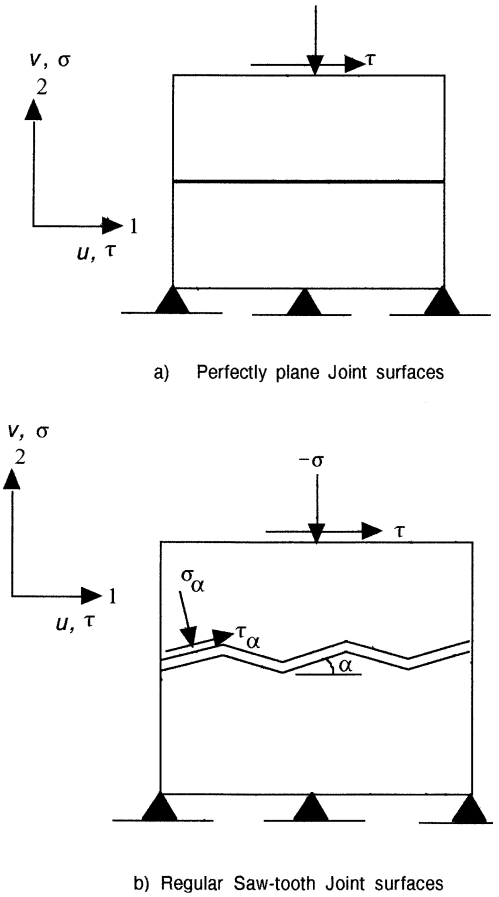

Figure 1. Joint model proposed by Patton[5]

By imposing the constraint that only shear traction can produce permanent deformation due to sliding, Michalowski and Mroz[28] proposed that, in the case of perfectly plane contact surface.

$$Q = |\tau| \tag{4}$$

In Patton's model shown in Figure 1, the asperities have regular angles of inclination α with respect to the horizontal direction. Along a typical asperity inclined at angle α, the relationship between the 'macro' values of the stresses τ and σ and the 'local' or 'micro' values of the stresses τ_α and σ_α can be obtained by appeal to local equilibrium at the inclined sliding plane, i.e.

$$\tau_\alpha = (\tau \cos\alpha + \sigma \sin\alpha)\cos\alpha \tag{5}$$

$$\sigma_\alpha = (\tau \cos\alpha - \sigma \sin\alpha)\cos\alpha \tag{6}$$

Movement will start along the asperity if according to equation (1)

$$|\tau_\alpha| = -\sigma_\alpha \tan\phi \tag{7}$$

and thus, the yield criterion for the saw-tooth joint model is

$$F = |\sigma \sin\alpha + \tau \cos\alpha| + \tan\phi(\tau \cos\alpha - \sigma \sin\alpha) \tag{8}$$

Similarly, the plastic potential function is defined as

$$Q = |\sigma \sin\alpha + \tau \cos\alpha| \tag{9}$$

Derivation of the elastoplastic stiffness matrix of the model by Plesha

In the formulation presented by Plesha,[1] sliding along the asperities is considered. When the magnitude of the applied shear stress is such that F, as defined in equation (8), is less than zero, only elastic deformations in the shear direction take place. Plastic or irrecoverable deformations in both shear and normal directions take place when $F = 0$. The total increment of relative displacement at the joint, in this case, is the sum of an elastic and a plastic component; i.e.

$$\mathrm{d}u_i = \mathrm{d}u_i^{\mathrm{e}} + \mathrm{d}u_i^{\mathrm{p}} \tag{10}$$

When plastic displacements occur, the asperities of the joint are damaged, resulting in a decrease of the asperity angle. Plesha[1] assumes that the asperity angle decreases as an exponential function of the plastic work produced by shear

$$\alpha = \alpha_0 \exp\left(- \int_0^{W^{\mathrm{p}}} c \, \mathrm{d}W^{\mathrm{p}} \right) \tag{11}$$

where α_0 is the original asperity angle, c is a degradation coefficient and W^{p} is the plastic work produced by the shear stress

$$W^{\mathrm{p}} = \int \tau \, \mathrm{d}u_1^{\mathrm{p}} \tag{12}$$

where $\mathrm{d}u_1 = \mathrm{d}u$ is the relative joint shear displacement.

From the consideration of asperity degradation, strain softening behaviour will now occur at the joint during plastic deformation, i.e. both the yield surface and the potential surface, as defined respectively, by equations (8) and (9), will shrink in the τ–σ stress space. Both F and Q will now be functions of not only τ and σ but also of the plastic work defined by equation (12) (i.e. $F = F(\tau, \sigma, W^{\mathrm{p}})$ and $Q = Q(\tau, \sigma, W^{\mathrm{p}})$.

The increment of stress $\mathrm{d}\sigma_i$ is related to the increment of elastic displacement at the joint by

$$\mathrm{d}\sigma_i = D_{ij} \, \mathrm{d}u_j^{\mathrm{e}} \tag{13}$$

where D_{ij} is the elastic stiffness matrix (with elements having units of Pa/m in SI units).

Following conventional procedures applicable to the mechanics of elastoplastic solids[29] and interface plasticity,[1,30] it can be shown that

$$\mathrm{d}\sigma_i = D_{ij}^{\mathrm{ep}} \, \mathrm{d}u_j \tag{14}$$

where D_{ij}^{ep} is the elastoplastic stiffness matrix, given by

$$D_{ij}^{\mathrm{ep}} = D_{ij} - \frac{1}{\psi - H} \frac{\partial Q}{\partial \sigma_k} D_{ik} D_{mj} \frac{\partial F}{\partial \sigma_m} \tag{15}$$

and

$$\lambda = \frac{1}{\psi - H} \frac{\partial F}{\partial \sigma_i} D_{ij} \, \mathrm{d}u_j \tag{16}$$

$$\psi = \frac{\partial F}{\partial \sigma_k} D_{km} \frac{\partial Q}{\partial \sigma_m} \tag{17}$$

$$H = \frac{\partial F}{\partial W^{\mathrm{p}}} \tau \frac{\partial Q}{\partial \tau} \tag{18}$$

With explicit expressions of F and Q as given in equations (8) and (9), the elastoplastic stiffness matrix could be explicitly formulated as a function of the current stress level by performing the differentiations in equation (18).

Parameters of Plesha's model

The parameters required for the model proposed by Plesha[1] are the elastic stiffness constants, the degradation factor c, the initial asperity angle α_0 and the friction angle ϕ. Usually, it is assumed that

$$D_{11} = k_{\mathrm{s}} \quad D_{22} = k_{\mathrm{n}} \quad D_{12} = D_{21} = 0$$

where k_{s} and k_{n} are, respectively, the elastic shear and normal stiffness.

Plesha[1] estimated the parameters of the model by calibrating the results of experimental data derived from shear test under constant normal stress. We propose here that these parameters can also be estimated from Barton's empirical coefficients JRC and JCS. First, we note that the surface asperities in real joints do not follow a regular pattern as idealized by Patton[5] and Plesha[1] (Figure 2). Several orders of irregularities exist, and each order will be activated depending on the size of the sample and the magnitude of the normal stress. For high normal stresses, the higher-order asperities will be subjected to through-shear and sliding will occur only along the lower-order asperities (with lower effective angle α). Similarly, for larger joint samples, the lower-order asperities will be activated. It is clear from the above discussion that the effective asperity angle for real joints will depend on the size of the joint, the magnitude of the normal stress, and the strength of the joint wall material. These factors could be taken into account if one adopts the Barton–Bandis[8,9] empirical expression for the peak shear envelope

$$|\tau| + \sigma \tan\left(\mathrm{JRC}\,\mathrm{Log}_{10}\left(\frac{\mathrm{JCS}}{\sigma}\right) + \phi\right) = 0 \tag{19}$$

Noting that equation (8) can be rewritten as

$$\begin{aligned} |\tau| + \sigma \tan(\phi + \alpha) &= 0 \quad \text{when } \sigma \sin\alpha + \tau\cos\alpha > 0 \\ |\tau| + \sigma \tan(\phi - \alpha) &= 0 \quad \text{when } \sigma \sin\alpha + \tau\cos\alpha < 0 \end{aligned} \tag{20}$$

and by comparing equations (19) and (20), one can write

$$\alpha = \mathrm{JRC}\,\mathrm{Log}_{10}\left(\frac{\mathrm{JCS}}{\sigma}\right) \tag{21}$$

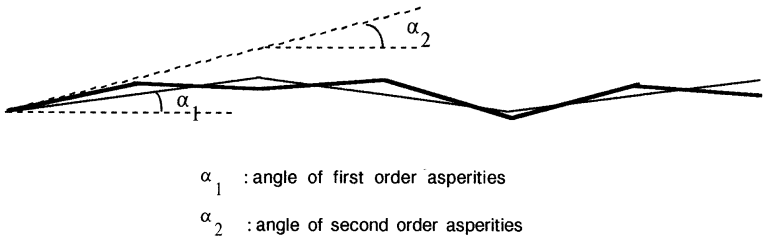

Figure 2. Schematic illustration of the many orders of asperities for real joints

The coefficients JRC (dimensionless) and JCS (MPa) and the friction angle ϕ can be easily estimated from two tests[8,9]: the tilt test and the Schmidt hammer test. To determine ϕ, an artificial clean joint is prepared by diamond-sawing of a rock specimen containing the real joint, and sandblasting the surfaces. The jointed rock specimen is then tilted until sliding occurs along the clear joint. The tilt angle measured will be equal to ϕ_b. The angle ϕ_b reflects pure friction resistance of clean (unweathered) planar surfaces. The friction angle ϕ for the real joint also reflects pure frictional behaviour. Nevertheless, the real joint contains gouge material originating from the failure of surface asperities. From the results of 135 shear tests on natural joints, Barton and Choubey[8] have proposed the following empirical relationship between ϕ and ϕ_b, i.e.

$$\phi = (\phi_b - 20) + 20(r/R) \tag{22}$$

where, R and r are rebound value (m) from the Schmidt hammer test performed, respectively, on a clean, *dry* unweathered surface and on a *wet* joint surface. JCS, the joint wall compressive strength is obtained from a simple empirical relation with the Schmidt rebound value

$$\mathrm{Log}_{10}\,\mathrm{JCS} = 0{\cdot}00088\rho R + 1{\cdot}01 \tag{23}$$

where JCS is in MPa, ρ is the unit weight of the dry rock in kN/m^3.

The value of JRC, on the other hand, is determined from the tilt test, by using equation (19)

$$\mathrm{JRC} = (\beta - \phi r)/\log(\mathrm{JCS}/\sigma_0) \tag{24}$$

where β is the tilt angle when sliding occurs and σ_0 is the self-weight induced normal stress acting on the joint, at the instant of sliding.

The parameters JRC and JCS are both scale-dependent. Bandis *et al.*[9] proposed the following empirical relations:

$$\mathrm{JRC} = \mathrm{JRC}_0\left(\frac{L}{L_0}\right)^{-0{\cdot}02\,\mathrm{JRC}_0} \tag{25}$$

$$\mathrm{JCS} = \mathrm{JCS}_0\left(\frac{L}{L_0}\right)^{-0{\cdot}03\,\mathrm{JRC}_0} \tag{26}$$

where JRC_0 and JCS_0 are laboratory-scale values, for joints with normal size $L_0 = 100$ mm and JRC and JCS are values for larger samples, of size L.

Bandis *et al.*[9] also experimentally observed that u_{peak}, the shear displacement corresponding to the peak shear stress τ_{peak}, under constant normal stress conditions, can be considered to be

independent of the normal stress but is scale dependent, i.e.

$$u_{\text{peak}} = \frac{L}{500}\left(\frac{\text{JRC}}{L}\right)^{0\cdot 33} \tag{27}$$

Assuming linear elastic response of the joint up to the peak shear stress, we can obtain, from equations (19) and (27), the elastic shear stiffness k_s as follows:

$$k_s = \frac{|\tau_{\text{peak}}|}{u_{\text{peak}}} = \frac{\sigma \tan(\text{JRC}\,\text{Log}_{10}(\text{JCS}/\sigma) + \phi)}{(L/500)/(\text{JRC}/L)^{0\cdot 33}} \tag{28}$$

The remaining parameter required for the model proposed by Plesha[1] is the normal stiffness k_n. This parameter can be determined by performing compression tests on jointed rock specimens. The most comprehensive experimental investigations on the normal closure behaviour of joints under applied normal stresses are due to Bandis *et al.*[9] In these studies, 64 pairs of specimens, with a wide range or rock types and surface roughness were tested. Each pair of specimens consists of one jointed specimen and one unjointed specimen. Normal compression tests were performed on both specimens. The deformation of the unjointed specimen was subtracted from the deformation of the jointed specimen in order to obtain the net deformation properties of the joint. Typically, several cycles of loading–unloading were performed. Strong hysteresis is observed for the first few cycles and this hysteresis progressively disappears with the number of cycles. The third or fourth cycle is generally considered to be representative of *in situ* conditions. The normal stress-closure curves have the shape of steep hyperbolae. Several authors[9,10] adopt hyperbolic relations to describe these experimental curves. For example, Bandis *et al.*[9] proposed the following hyperbolic relationship:

$$\sigma = k_{\text{ni}} \frac{v}{1 - v/v_{\text{m}}} \tag{29}$$

where k_{ni} is the normal stiffness at zero normal stress, and v_{m} is the maximum closure of the joint.

The normal stiffness at any level of normal stress is then

$$k_{\text{n}} = \frac{\text{d}\sigma}{\text{d}v} = k_{\text{ni}}\left(1 - \frac{\sigma}{v_{\text{m}}k_{\text{ni}} + \sigma}\right)^{-2} \tag{30}$$

The parameters k_{ni} and v_{m} that enter into equation (30) are best determined by performing compression tests on jointed rock samples.

HYDRAULIC BEHAVIOUR OF A JOINT

The parallel plate model, developed by the application of the Navier–Stokes equation for laminar incompressible flow between two parallel smooth plates, is usually used to calculate the permeability k of the fracture (see, e.g. Reference 4), i.e.

$$k = e_{\text{h}}^2/12 \tag{31}$$

where e_{h} is the hydraulic aperture of the joint.

Since natural fractures are quite dissimilar to ideal parallel plates, the hydraulic aperture of the fracture is not equal to its mechanical aperture. Barton[24] proposed the following empirical

relationship to estimate the hydraulic aperture from the mechanical aperture

$$e_h = \frac{e_m^2}{JRC^{2\cdot5}} \tag{32}$$

where e_h is in μm, e_m (also in μm) is the mechanical aperture of the joint.

Elliot *et al.*[25] and Witherspoon *et al.*[26] proposed a linear relationship between the hydraulic and mechanical apertures

$$e_h = e_{h0} + f\Delta e_m \tag{33}$$

where e_{h0} is the initial hydraulic aperture, Δe_m is the variation in mechanical aperture due to the combined effects of compression and shear as discussed in the above section, and f is a proportionality factor. Benjelloun[4] experimentally confirmed the validity of equation (33) and found that f varies between 0·5 to 1. This factor comes from the roughness of the joint surfaces. A factor $f = 1$ applies to the limiting ideal case of parallel smooth plates; this situation prevails only when the joint is relatively open, with apertures of the order of mm. For most other cases, $f < 1$. The geometry of the flow path has an important influence on f. For rectilinear laminar flow, f is generally close to 0·8 and for radial flow, f close to 0·5 (see Reference 4).

In this paper, we adopt the linear relationship between the hydraulic and mechanical apertures given in equation (33). During the shearing of a joint, dilation occurs as discussed in the previous section. This results in an increase of the mechanical aperture Δe_m. Equations (31) and (33) indicate that the permeability of the joint should increase with joint shear. Bandis *et al.*[2] experimentally observed such an increase in permeability. Nevertheless, at later stages of shearing, the permeability of the joint decreases. This observation is attributed to the effect of gouge production due to asperity breakage, that could not be explained by the existing models, similar to those defined in equations (32) and (33). In order to simulate the effect of gouge production on the joint permeability, we assume that this effect is related to the total plastic work due to shear. Adopting the form of the relation proposed by Plesha[1] [equation (11)], we assume that the factor f in equation (33) is related to the plastic work produced by the shear forces according to the following equation:

$$f = f_0 \exp\left(- \int_0^{W^p} c_f \, dW^p \right) \tag{34}$$

where c_f is a gouge production factor. It is very likely that the additional parameters f_0 and c_f introduced in this section can be empirically related to JRC, JCS and σ. A detailed experimental program will be needed in order to arrive at specific correlations.

SIMULATION OF LABORATORY EXPERIMENTS

The above joint model was implemented in the finite element code FRACON.[31,32] The FRACON code is a finite element code capable of simulating coupled thermal–hydrological–mechanical processes in fractured media. The governing equations are derived from the classical theory of consolidation developed by Biot (see e.g. Reference 39). Eight-noded isoparametric elements are used to simulate intact blocks of the geological medium, while special six-noded elements are used to simulate discontinuities such as joint. The FRACON code will now be used to simulate typical laboratory experiments on rock joints.

Shear under constant normal stress

Most laboratory experiments on joints are performed under constant normal stress conditions. These conditions apply mainly to geomechanical problems associated with rock slope stability, where the focus is on the analysis of the sliding movement of rock blocks near the surface of a slope. The constant normal stresses across the joints between these blocks is due to the weight of the blocks themselves.

We show here the simulation of experiments involving shear under constant normal stress performed by Skinas *et al.*[18] The tests were conducted on 15 cm × 10 cm model joints. These joints were cast from natural joint surfaces, using a brittle, artificial material consisting of a sand-barytes-cement mixture. Skinas *et al.*[18] presented experimental results for joints with the following properties:

$$\text{JRC} = 9, 12, 15 \text{ and } 18 \quad \text{JCS} = 28 \text{ MPa} \quad \phi = 37^\circ$$

We performed the simulation with the FRACON code of the tests performed on the joint with JRC = 9. The input data required for the FRACON code are:

$$\text{JRC} = 9 \quad \text{JCS} = 28 \text{ MPa} \quad \phi = 37^\circ$$

Three levels of normal stress are considered: 1, 2 and 5 MPa. In order to obtain a good agreement between the calculated and experimental results (for shear stress versus shear displacement) different values of the asperity degradation coefficient c are assumed for different normal stress values: $1{\cdot}1 \times 1^{-4}$ m/N ($\sigma = 1$ MPa), $0{\cdot}4 \times 10^{-4}$ m/N ($\sigma = 2$ MPa), $0{\cdot}25 \times 10^{-4}$ m/N ($\sigma = 5$ MPa). Figure 3 shows that the asperity degradation coefficient decreases with increasing compressive normal stress. This observation is consistent with experimental results obtained by Benjelloun.[4] However, Hutson and Dowding[34] and Qiu *et al.*[35] observed the reverse trend.

The finite element model consists of a single joint element (Figure 4). Constant normal stresses are applied on the element, and shear displacements are imposed at the appropriate nodes.

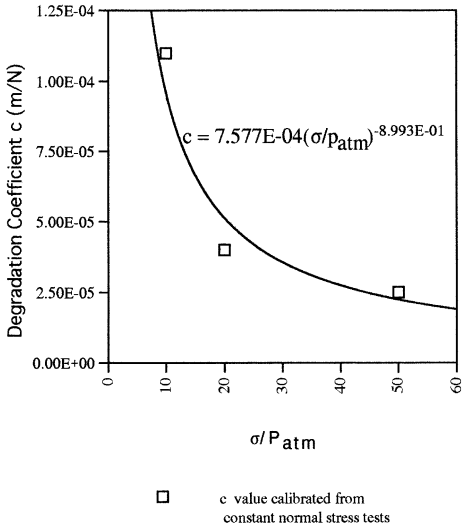

Figure 3. Variation of asperity degradation coefficient with normal stress

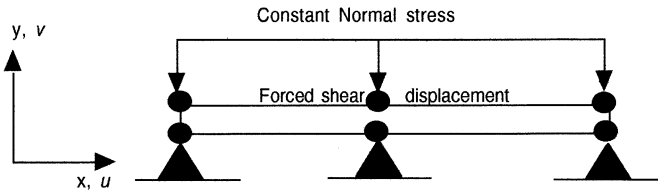

Figure 4. Finite element model for joint shear under constant normal stress condition

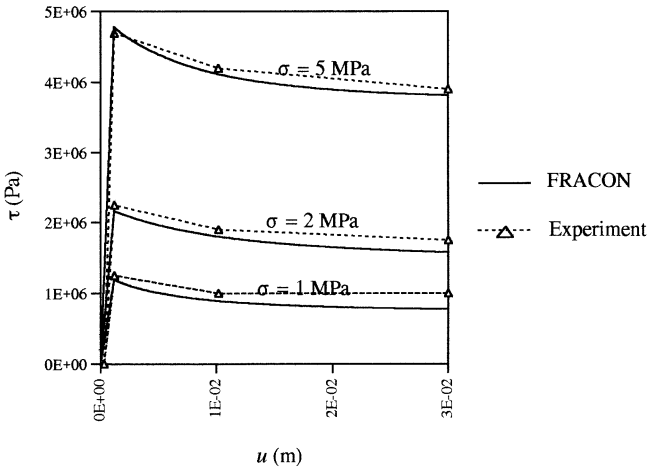

Figure 5. Shear under constant normal-stress—shear stress vs. shear displacement

The results for shear stress versus shear displacement are shown in Figure 5. A close fit was obtained between the results derived from the numerical modelling and the experimental results. Figure 5 shows that the shear strength of the joint increases with the normal stress level, at the same time the joint becomes more brittle (i.e. strain softening becomes more pronounced). The displacement corresponding to the peak shear stress does not depend on normal stress level, but only on the size of the joint sample [cf. equation (31)]. These observations are also consistent with experimental results obtained by other researchers (e.g. References 4, 8, 9).

The joint dilation due to shear is shown in Figure 6. For a value of the normal stress of 1 MPa, the FRACON code overpredicts dilation by approximately 15 per cent when compared to the experimental results. This might be due to an inherent feature of the implementation of the model by Plesha[1] into the FRACON code. This model does not allow the joint surfaces to approach one another as the asperities are degraded. Plesha[33] included this damage deformation in a recent version of his model. The FRACON code nevertheless correctly predicts decreasing dilation with increasing normal stress, as found experimentally by numerous researchers (e.g. References 4, 8, 9). No experimental data were given by Skinas *et al.*[18] for dilation at normal stress values of 2 MPa and 5 MPa.

Figures 7–9 illustrate the effects of degradation on the joint behaviour, for a typical case (normal stress of 1 MPa). From Figure 7, it may be observed that the joint would behave in an

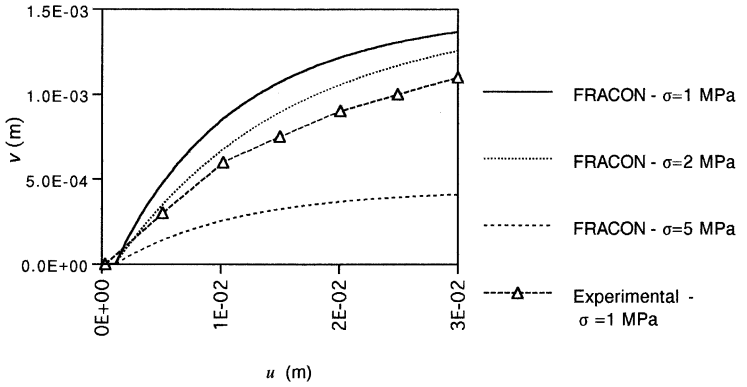

Figure 6. Shear behaviour under constant normal stress conditions—joint dilation

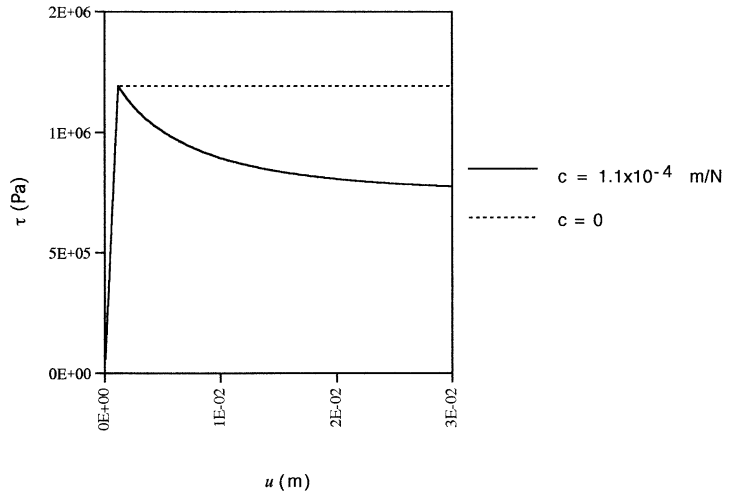

Figure 7. Effects of degradation on shear stress

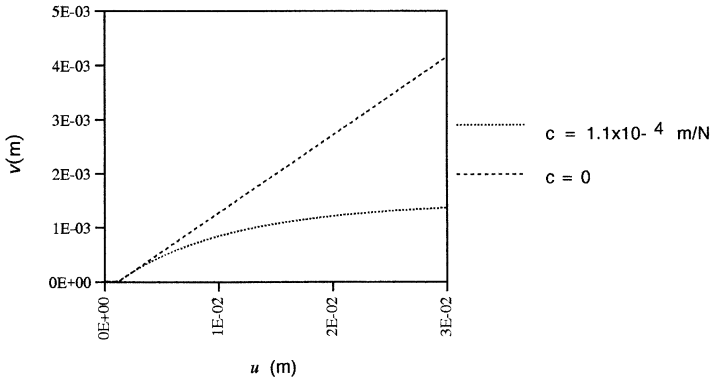

Figure 8. Effects of degradation on dilation

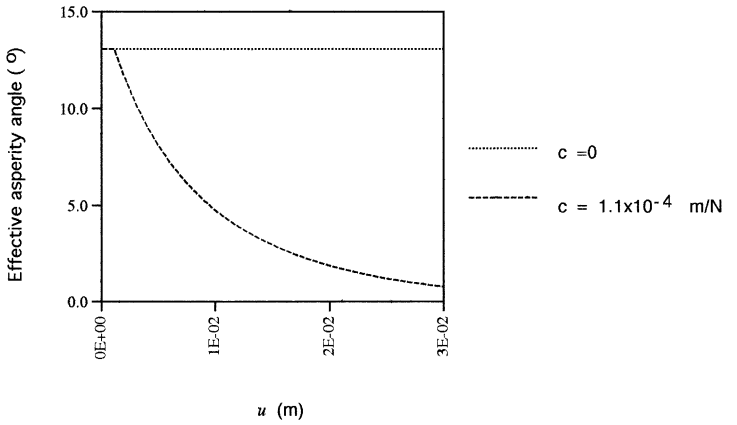

Figure 9. Effects of degradation on the asperity angle

elastic–perfectly plastic fashion if no degradation takes place ($c = 0$). For this latter case, Figure 8 shows that dilation of the joint will take place indefinitely at a constant rate, while this rate would decrease and tend to zero if degradation is considered. Figure 9 shows that due to degradation (case when $c = 1{\cdot}1 \times 10^{-4}$ m/N), the asperity angle gradually tends to zero.

Shear under constant stiffness

Skinas *et al.*[18] also presented results of shear tests performed under constant external stiffness conditions. The external stiffness variations are achieved by incorporating springs of different stiffnesses which restrain normal movement of the joint samples. The joints are then sheared by the application of a force in the shear (horizontal) direction. These test conditions correspond to the situation that can be encountered in rock joints located at some depth within a rock mass. The tendency for dilation of the joints will be restricted by the stiffness of the surrounding rock mass. We perform simulation of these tests under external spring stiffnesses of 1·03, 3·33 and 13·33 GPa/m and an initial normal stress of 1 MPa. The joint sample has properties similar to those described in the previous section. In particular, the degradation coefficient is assumed to vary according to a power law of the normal stress as shown in Figure 3. The coefficients of this power function are estimated by the curve of best fit derived from the discrete calibrated values obtained from the simulation of the shear tests under constant normal stress. The normal stiffness of the joint, which does not play a role in the previous case, has to be taken into account under the current conditions. In the absence of experimental data, we have assumed that k_n is given by equation (30), with $k_{ni} = 2 \times 10^9$ Pa/m and $v_m = 8 \times 10^{-4}$ m.

The finite element model used in the FRACON code is shown in Figure 10. The stiffness of the springs is simulated by an eight-noded element which has elastic properties and height H equivalent to the corresponding spring stiffness K_n:

$$H = 1 \text{ m}, \quad E = 1{\cdot}033 \text{ GPa (for } K_n = 1{\cdot}033 \text{ GPa/m)},$$

$$3{\cdot}33 \text{ GPa } (K_n = 3{\cdot}33 \text{ GPa/m}), \; 1{\cdot}33 \text{ GPa } (K_n = 13{\cdot}33 \text{ GPa/m}), \quad \nu = 0$$

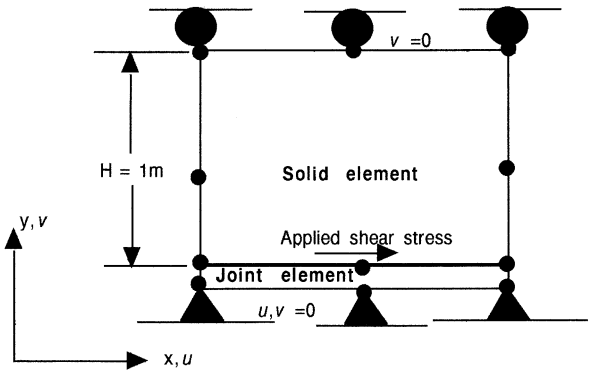

Figure 10. Finite element model for shear under a constant normal stiffness condition

Shear stress and normal stress are shown in Figure 11. Reasonable agreement was obtained between the results derived from the FRACON code and the experimental data. Both sets of results show that the stiffness of the external springs, because of its restraining influence on the dilation, results in a strengthening of the joint. The pre-yield behaviour of the joints is essentially the same for all values of external stiffness. The post-yield behaviour shows a completely different picture. For an external stiffness of zero (which can be interpreted as a constant normal stress condition), the shear stress decreases due to asperity degradation. This is the strain softening -behaviour discussed in the previous section. When the external stiffness increases, strain hardening of the joint occurs. Both the shear and normal stress increase when shearing continues beyond the yield point, as shown in Figure 11.

Effects of shear on joint permeability

Bandis *et al.*[2] presented results of hydromechanical experiments performed on rock joints. The experimental setup is a biaxial cell (Figure 12). The joint sample is first compressed without shear by increasing σ_1 and σ_2 in equal increments. The joint is then sheared by maintaining one load constant and increasing the other. At specific values of shear displacement, the permeability of the joint was determined by injecting water through the joint and measuring the flow rate. Bandis *et al.*[2] record the evolution of the joint permeability with increasing shear displacement (Figure 13). Although both the normal and shear stresses vary during the experiment, Bandis *et al.*[2] assume constant normal stress conditions to simulate the evolution of joint permeability. The assumed constant normal stress is the average value of the actual normal stress. In this paper, we also computationally simulate the experiment by assuming constant normal stress conditions. The joint material is gneiss for which Bandis *et al.*[2] give the following properties:

$$\text{JRC} = 7 \quad \text{JCS} = 110\ \text{MPa} \quad \text{joint length: } L = 0{\cdot}15\ \text{m} \quad \text{average normal stress: } 1{\cdot}5\ \text{MPa}$$

The finite element model used in the FRACON simulation is similar to that shown in Figure 4. The joint properties given above are used as input to the simulation. In addition, an asperity degradation factor $c = 1{\cdot}5 \times 10^{-4}\ \text{m/N}$ was assumed. When sheared, the joint dilates. The dilation calculated by FRACON is shown in Figure 14. This dilation is accompanied initially by

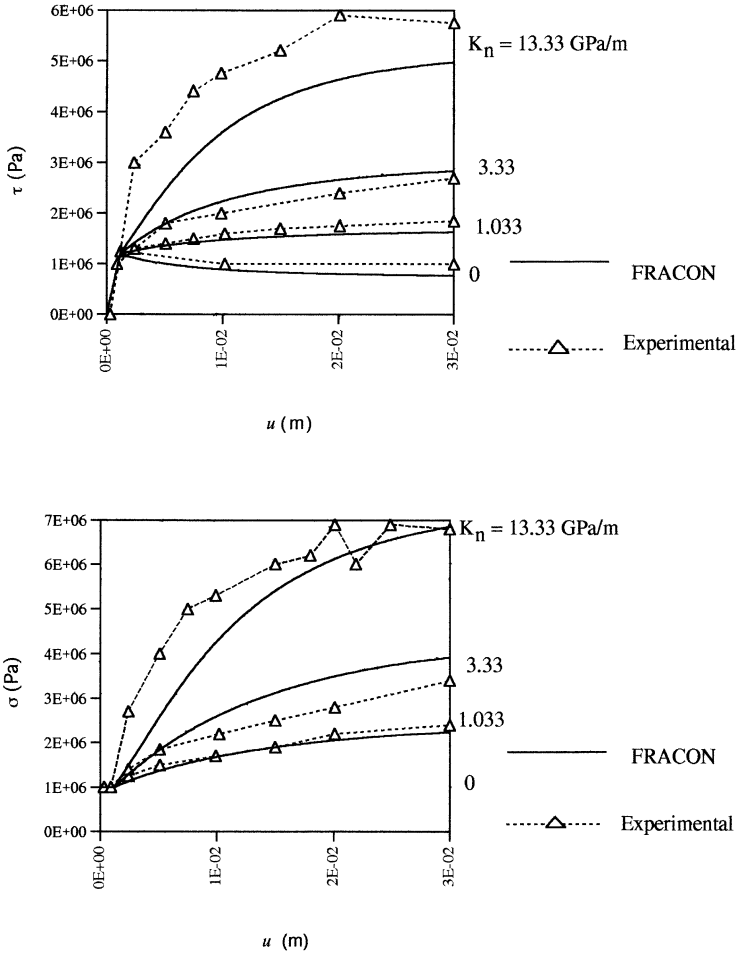

Figure 11. Joint behaviour under constant normal stiffness conditions

a corresponding increase in the permeability of the joint (Figure 13). However, this permeability later decreases due to gouge production by joint asperity breakage. Bandis *et al.*[2] could not simulate this permeability decrease (Figure 13), using Barton's[24] model [cf. equation (32)]. The FRACON code simulation, with a gouge production factor $c_f = 0$, produces results similar to those presented by Bandis *et al.*[2]. Assuming $c_f = 0{\cdot}001$ m/N, the trends in the permeability variations predicted by the FRACON code agree relatively well with the experimental results. Most importantly, the tendency for the reduction in the permeability of the joint with increasing shear is correctly predicted.

Scale effects

Bandis *et al.*[9] studied scale effects on joints by making identical pairs of replicas of natural joints, using a brittle model material. These artificial joint samples were tested full-size or were divided

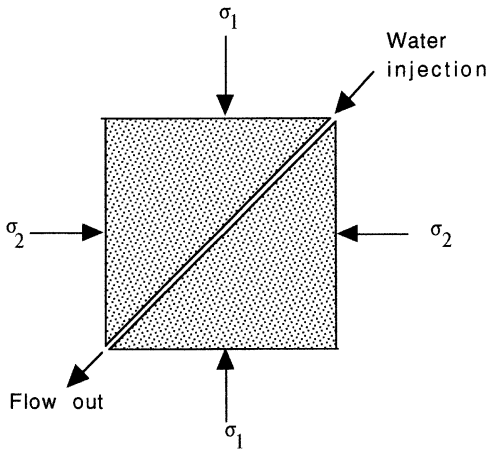

Figure 12. Schematics of the hydromechanical experiments performed by Bandis *et al.*[2] and Makurat *et al.*[3]

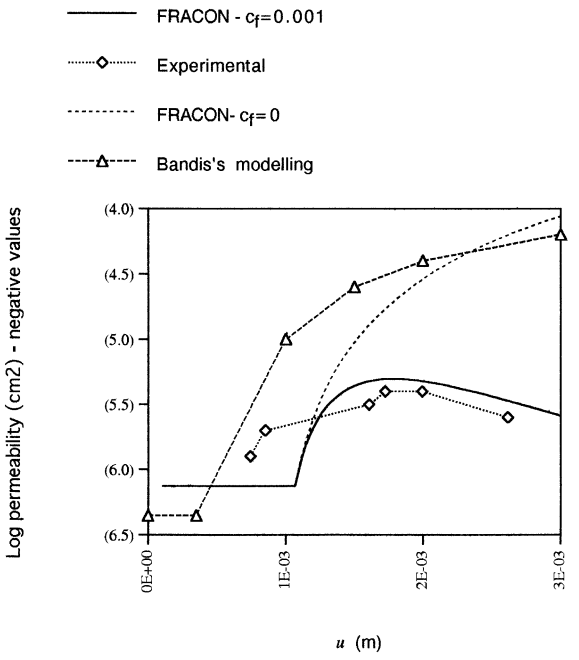

Figure 13. Hydromechanical experiments—effects of shear on joint permeability

into smaller samples for testing separately. In these experiments shear tests were performed under constant normal stress conditions.

In this study, the scale effects in the tests conducted by Bandis *et al.*[9] are simulated by using the properties given in their studies:

$$L_0 = 6\ \text{cm} \quad \text{JRC}_0 = 16{\cdot}7 \quad \text{JCS}_0 = 2\ \text{MPa} \quad \text{normal stress} = 24{\cdot}5\ \text{kPa}$$

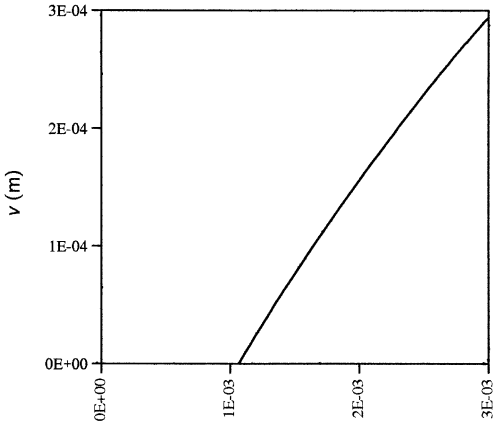

Figure 14. Hydromechanical experiments—shear dilation calculated via the FRACON code

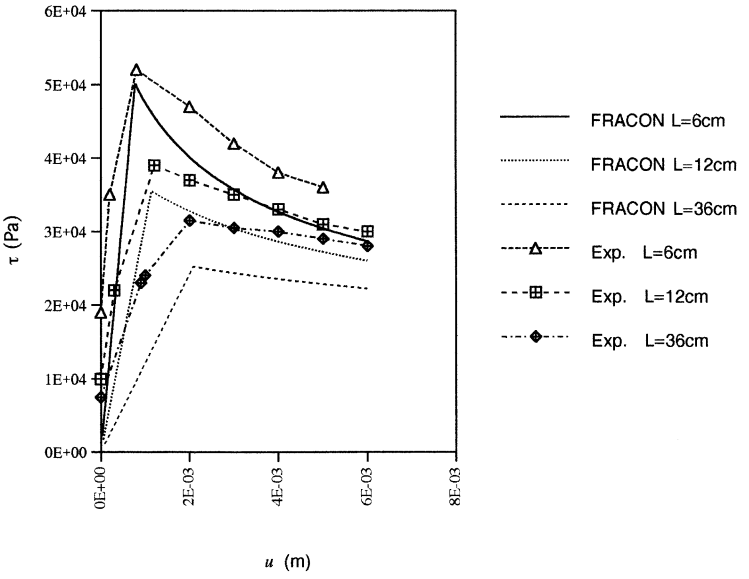

Figure 15. Scale effects on joint shear

Scale effects are simulated with the FRACON code by using the empirical equations (25) and (26). The finite element mesh used in the study is similar to the one shown in Figure 4.

Figure 15 shows that the FRACON code correctly predicts that with increasing size, strain softening is less pronounced, i.e. the joint behaviour becomes less brittle. With increasing size, the shear stiffness prior to failure decreases and the displacement required to reach the peak shear stress increases. The shear strength of the joint is somewhat underestimated by the numerical modelling, especially for the larger specimens.

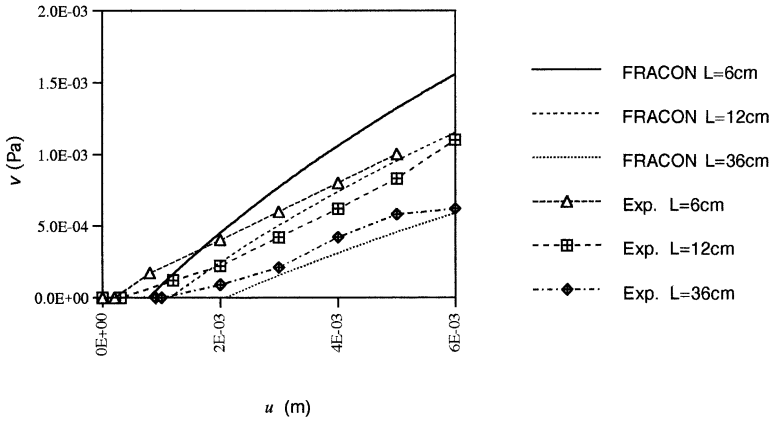

Figure 16. Scale effects on joint dilation

Figure 16 shows scale effects on joint dilation. The FRACON code correctly predicts a decrease in shear dilation with larger samples. The experimental data shows that dilation starts before the peak shear stress is attained. As can be seen in Figure 16, the model by Plesha[1] incorporated in the FRACON code assumes linear elastic behaviour in the pre-peak phase. Thus, dilation is predicted to start only after the attainment of the peak shear stress. As previously discussed, because no damage deformation is incorporated in the model, with the smaller joint samples, the FRACON code overpredicts the dilation value.

CONCLUSIONS

A joint model was implemented in a finite element code (FRACON) to simulate coupled thermal–hydrological–mechanical processes in fractured geological media. The stress–strain relationship of the joint was formulated using the classical incremental theory of plasticity applicable to non-linear interfaces. The geometry of the joint surfaces is idealized by a series of regular asperities with constant angle with respect to the shear direction. During shearing, the joint dilates as a result of ride up at the asperities. Also, the shearing process can result in breakage of the asperities, resulting in the decrease of the dilation rate and strain softening of the joint. Following the work by Plesha[1] it is assumed that asperity damage can be related to the plastic work of the shear stress and as a consequence the asperity angle is assumed to be a decaying exponential function of this plastic work of the shear stress at the joint. We have extended this concept to describe the hydraulic behaviour of the joint in the following manner. Dilation of a joint during shear leads to an increase of its permeability. On the other hand, gouge produced from breakage of the asperities would block the flow path and tends to decrease the joint permeability. The results of experimental work available in the literature indicate that shearing of the joint leads to an initial increase followed by a decrease of the joint permeability. Existing models do not allow for the prediction of this behaviour. In the present work, we assume that the increase in the hydraulic aperture is proportional to the increase in the mechanical aperture. The results of several experimental investigations in the literature have confirmed this assumption. These investigations also showed that the factor of proportionality f varies between

0·5 and 1·0 depending on the geometry of the flow direction. We assumed that gouge production is due to the plastic work from the shear stress, and thus the factor f is assumed to be a decaying exponential function of the plastic work.

The parameters of the proposed joint model could be back-calculated from shear tests under constant normal stress conditions with permeability measurement and normal closure tests. Alternatively, most of these parameters could be estimated from the empirical coefficients JRC and JCS. Using the latter approach, the effects of the normal stress on dilation and scale effects become integral aspects of the proposed model. The two parameters which could not be expressed as empirical functions of JRC and JCS at the present time are the asperity degradation factor, c, and the gouge production factor, c_f. In order to achieve such correlations, it is necessary to conduct an extensive series of experiments involving both natural and artificial joints.

The proposed joint model has been implemented in a finite element code (FRACON). The code was used to simulate several experiments: shear tests under constant normal stress and under constant normal stiffness conditions performed by Skinas *et al.*[8] and coupled shear-flow experiments performed by Bandis *et al.*[2] The model performs quite statisfactorily in simulating the trends observed in the above experiments. Scale effects, as evidenced from the experimental results of Bandis *et al.*,[9] are also correctly predicted by the proposed model. It is recognized that more sophisticated models, based on the classical theory of plasticity exist in the scientific literature. For example, the models proposed by Desai and Fishman[36] and Desai and Ma[37] allow for more accurate predictions of a wide range of laoratory tests, under a variety of test conditions. These models allow for an expanding yield function F in the stress space, include hardening and softening behaviours, and correctly predict the occurence of shear dilation before the peak stress state is attained. Nevertheless, the number of constants needed for these models becomes much more important. The model proposed in this paper on the other hand requires only a minimal number of parameters (JRC and JCS) which are easily measured in practice.

REFERENCES

1. M. E. Plesha, 'Constitutive models for rock discontinuities with dilatancy and surface degradation', *Int. J. Numer. Analyt. Meth. Geomech.*, **11,** 345–362 (1987).
2. S. Bandis, A. Makurat and G. Vik, 'Predicted and measured hydraulic conductivity of rock joints', *Proc. Int. Symp. on Fundamentals of Rock Joints*, Bjorkliden, Sweden, Balkema, 1985.
3. A. Makurat, N. Barton, N. S. Rad and S. Bandis, 'Joint conductivity variation due to normal and shear deformation', *Proc. Int. Symp. on Rock Joints*, Leon, Norway, Balkema, 1990.
4. Z. H. Benjelloun, 'Etude Experimentale et Modélisation du Comportement Hydromécanique des Joints Rocheux', Thèse de doctorat, Université Joseph Fourier, Grenoble 1, 1993.
5. F. D. Patton, 'Multiple modes of shear failure in rock', *Proc. 1st Congress of Int. Society of Rock Mech.*, Lisbon, **1,** 1966, 509–513.
6. B. Ladanyi and G. Archambault, 'Simulation of shear behaviour of a jointed rock mass', *Proc. 11th Symp. Rock. Mech.*, American Institute of Mechanical Engineers, New York, 1970.
7. J. C. Jaeger, 'Friction of rocks and stability of rock slopes', *Geotechnique* **21,** 97–134 (1971).
8. N. Barton and V. Choubey, 'The shear strength of rock joints in theory and practice', *Rock Mech.*, **10,** 1–54 (1977).
9. S. Bandis, A. C. Lumsden and N. Barton, 'Experimental studies of scale effects on the shear behaviour of rock joints', *Int. J. Rock Mech. Min. Sci. Geomech. Abst.*, **18,** 1–21 (1981).
10. R. E. Goodman, *Methods of Geological Enginering in Discontinuous Rocks*, West Publishing Company, New York, 1976.
11. R. E. Goodman and J. Dubois, 'Duplication of dilatancy in analysis of jointed rock', *J. Soil Mech. Found Div., ASCE* **SM4,** 399–422 (1972).
12. F. E. Heuze, 'Dilatant effects of rock joints', *Proc. 4th congress of Int. Society of Rock Mech.*, Montreux, Switzerland, 1979.
13. F. E. Heuze and T. G. Barbour, 'New models for rock joints and interfaces', *J. Geotechn. Eng., Div. Proc. ASCE*, **108, GT5,** 757–776 (1982).

14. W. Leichnitz, 'Mechanical Properties of rock joints', *Int. J. Rock Mech. Min. Sci. Geomch. Abst*., **22,** 313–321 (1985).
15. M. Boulon and R. Nova, 'Modelling of soil-structure interface behaviour—a comparison between elastoplastic and rate type laws', *Comput. Geotech*., **9,** 21–46 (1990).
16. G. Archambault, M. Fortin, D. E. Gill, M. Aubertin and B. Ladanyi, 'Experimental investigations for an algorithm simulating the effect of variable normal stiffness on discontinuities shear strength', *Proc. Int. Symp. on Roch Joints*, Loen, Norway, Balkema, 141–148, 1990.
17. B. Amadei and S. Saeb, 'Constitutive models of rock joints', *Proc. Int. Symp. on Rock Joints*, Loen, Norway, Balkema, 707–712, 1990.
18. C. A. Skinas, S. Bandis and C. A. Demiris, 'Experimental investigations and modelling of rock joint behaviour under constant stiffness', *Proc. Int. Symp. on Rock Joints*, Loen, Norway, Balkema, 301–308, 1990.
19. W. J. Roberds and H. H. Einstein, 'Comprehensive model for rock discontinuities', *J. Geotech. Engng*., *Proc. ASCE*, **104,** 553–569 (1978).
20. J. Ghaboussi, E. L. Wilson, and J. Isenberg, 'Finite element for rock joints and interfaces', *J. Soil Mech. Found. Div. Proc. ASCE*, **99,** 833–848 (1973).
21. K. Hsu-Jun, 'Nonlinear analysis of the mechanical properties of joint and weak intercalation in rock', *Proc. 3rd Int. Conf. on Num. Methods in Geomechanics*, Aachen, Germany, 523–532, 1979.
22. G. N. Pande and W. Xiong, 'An improved multilaminate model of jointed rock masses', in *Numerical Models in Geomechanics*, A. A. Balkema, Rotterdam, 218–226, 1982.
23. C. S. Desai and K. L. Fishman, 'Constitutive models for rocks and discontinuities', *Proc. 28th US Symp. on Rock Mechanics*, Tucson, Arizona, 609–619, 1987.
24. N. Barton, 'Modeling rock joint behavior from *in situ* block tests; implications for nuclear waste repository design', Office of Nuclear Waste Isolation *Report ONWI-208* 1982.
25. G. M. Elliot, E. T. Brown, P. I. Boodt and J. A. Hudson, 'Hydrochemical behaviour of joints in the Carmenelis granite, SW England', *Proc. Int. Symp. on Fundamentals of Rock Joints*, Bjorkliden, Sweden, A. A. Balkema, Rotterdam, 249–258, 1985.
26. P. A. Witherspoon, C. H. Amick, J. E. Gale and K. Iwai, 'Observations of a potential size effect in experimental determination of the hydraulic properties of fractures', *Water Resources Res.* **15,** 1142–1146 (1979).
27. R. M. Stesky, W. F. Brace, D. K. Riley and P. Y. E. Robin, 'Friction in faulted rock at high temperature and pressure', *Tectonophysics*, **23,** 177–203 (1974).
28. R. Michalowski and Z. Mroz, 'Associated and non-associated sliding rules in contact friction problems', *Arch. Mech*., **30,** 259–276 (1978).
29. C. S. Desai and H. J. Siriwardane, *Constitutive Laws for Engineering Materials with Emphasis on Geologic Materials*, Prentice-Hall, Englewood Cliffs, NJ 07632, 1984.
30. A. P. S. Selvadurai and M. Boulon (eds.), *Mechanics of Geomaterial Interfaces*, *Studies in Applied Mechanics* Vol. 42 Elsevier, Amsterdam, The Netherlands, 1995.
31. A. P. S. Selvadurai and T. S. Nguyen, 'Finite element modeling of consolidation of fractured porous mdeia', *Proc. 1993 Canadian Geotech. Conf.* 79–88, 1993.
32. T. S. Nguyen and A. P. S. Selvadurai, 'Modelling of thermal consolidation of sparsely fractured rock in the context of nuclear waste management', A. P. S. Selvadurai (ed.) *Mechanics of Poroelastic Media*, Kluwer, Dordrecht, The Netherlands, 159–180, 1996.
33. M. E. Plesha, 'Rock joints: theory, constitutive equations', in A. P. S. Selvadurai and M. Boulon (eds.) *Mechanics of Geomaterial Interfaces*, Elsevier, 375–393, 1995.
34. R. W. Hutson and C. H. Dowding, 'Joint asperity degradation during cyclic shear', *Int. J. Rock Mech. Mining Sci. Geomech. Abstr*., **27,** 109–119 (1990).
35. X. Qiu, M. E. Plesha, B. C. Haimson and X. Huang, 'An investigation of the mechanics of rock joints—part II, analytic investigation', *Int. J. Rock Mech. Mining Sci. Geomech. Abstr*., **30,** 271–287 (1993).
36. C. S. Desai and K. L. Fishman, 1991, 'Plasticity-based constitutive model with associated testing for joints', *Int. J. Rock Mech. Min. Sci. Geomech. Abstr*., **28,** 15–26 (1991).
37. C. S. Desai and Y. Ma, 1992, 'Modelling of joints and interfaces using the disturbed-state concept', *Int. J. Num. Analy. Meth. Geomech*., **16,** 623–653 (1992).
38. M. J. Boulon, A. P. S. Selvadurai, Z. H. Benjelloun and B. Feuga, 'Influence of rockjoint degradation on hydraulic conductivity, *Int. J. Rock Mech. Min. Sci*., *Geomech. Abstr*., **30,** 1311–1317 (1993).
39. A. P. S. Selvadurai (ed.) *Mechanics of Poroelastic Media*, Kluwer, Dordrecht, The Netherlands, 1996.

.

